PHYSICAL REVIEW B VOLUME 23, NUMBER 10 15 MAY 1981

Electronic structure of amorphous transition-metal alloys

J. Kübler
Abteilung für Physik, Ruhr-Universität Bochum, 4630 Bochum, Germany

K. H. Bennemann
Theoretische Physik, Freie Universität Berlin, 1000 Berlin 33, Germany

R. Lapka, F. Rösel, P. Oelhafen, and H.-J. Güntherodt
Institut für Physik, Universität Basel, Basel, Switzerland
(Received 18 July 1980)

In order to understand the electronic structure of transition-metal glasses the electronic density of states of corresponding ordered close-packed compounds have been calculated using the self-consistent augmented-spherical-wave method. Comparison of our band calculations and photoemission spectra of various glassy alloys suggest that the essential features of the electronic structure are very similar in glassy alloys and corresponding ordered close-packed alloys. In addition, core-level energy shifts are calculated and compared with experimental results. We explain the observed changes in the core-level line-shape asymmetries. Finally, we discuss the dependence of the thermal stability of transition-metal glasses on the number of d electrons and heats of formation.

I. INTRODUCTION

The electronic structure of transition-metal alloys and how it determines the alloy cohesion[1] and how it relates to the possibility to form glassy alloys[2] is of particular interest. Recently, it has become possible to form many glassy transition-metal alloys of type $A_{1-x}B_x$, such as $Zr_{1-x}Cu_x$, $Zr_{1-x}Ni_x$, etc., and thus more and new information on these transition-metal alloys has become available.

Photoemission experiments have shown for a series of amorphous transition-metal alloys that the constituent d-electron density of states $N(\epsilon)$ changes considerably upon alloying.[3,4] In particular, it has been observed that the d-band centers ϵ_d shift. This shift depends on alloy composition and on the valence difference of the alloy constituents. The latter dependence is approximately linear. Furthermore, in the alloy series $Zr_{1-x}Cu_x$, $Zr_{1-x}Pd_x$, etc., the Cu, Pd, etc., d bands become narrower and nearly Gaussian-like in shape. In the alloy series $Zr_{1-x}Ni_x$, $Zr_{1-x}Pd_x$, and $Zr_{1-x}Pt_x$, for example, one observes[4] that the d-band center of Ni, Pd, and Pt moves further away from the Fermi energy ϵ_F as one goes from Ni to Pd to Pt. For all the alloys, one observes shifts for the core-state energies and changes of their line shapes. The ability to form glasses and the glass temperature T_g is observed[5] to increase similarly as the heat of formation for alloys of type $Zr_{1-x}B_x$ for increasing valency of the B transition-metal atoms.

In the following we explain these experimental results in terms of usual alloy theory. In view of the lack of methods to calculate the electronic structure of an amorphous alloy, we take advantage by using the powerful methods developed for the crystalline state. We present density-of-states (DOS) results obtained by self-consistent augmented-spherical-wave (ASW)-type band-structure calculations for ordered (hypothetical) intermetallic compounds of the same (or nearly the same) stoichiometry as the glassy alloys. By comparing these results with photoemission spectra of related glassy alloys, we argue that the DOS and the electronic configuration with regard to the d electrons are similar for amorphous and ordered transition-metal alloys. In addition, these calculations give information on the partial DOS, which are not accessible by photoemission spectroscopy. Also, we have calculated the core-level binding energy shifts by taking into account the electronic valence-band structure. The results are compared with experimental results presented here for the first time. The observed changes in the core-level line-shape asymmetries on alloying are explained.

The results of the calculations are presented in Sec. II and compared with experimental data. In Sec. III we discuss the results. In particular, this section illuminates the underlying physics of the electronic behavior of glassy transition metals. Finally, we discuss the dependence of glass-forming ability and stability on heats of formation and electronic structure.

II. ELECTRONIC STRUCTURE OF TRANSITION-METAL ALLOYS

The main subject of this paper is the electronic properties of glassy transition-metal alloys con-

sisting of transition-metal atoms only. We focus our attention first on their densities of states, shifts of the core level, and changes of their line shapes.

A. Densities of states

We compare in Figs. 1–5 for various transition-metal alloys, results for the density of states $N(\epsilon)$ obtained by photoemission experiments[4] (marked "UPS" in the figures) and band calculations referring to crystalline compounds of type AB or A_3B.

The underlying band calculations were performed by the ASW method.[6] The calculations are self-consistent, using the local functional density theory of Hedin and Lundqvist.[7] For $PdZr_3$, $CuZr_3$, and $FeZr_3$, we use Cu_3Au-type symmetry with lattice constants $a = 4.151$ Å, $a = 4.110$ Å, and $a = 3.730$ Å, respectively. For NiNb we assume both CsCl- and CuAu-type symmetry with $a = 2.982$ Å and $a = 3.757$ Å, respectively. This should indicate or illustrate how sensitively $N(\epsilon)$ responds to changes in the local atomic order, to changes in the coordination number and atomic distances for which variations are expected in the amorphous alloys. The lattice constants were estimated using atomic volumes of the constituent metals. No attempt was made to determine the lattice constants by minimizing the total energy. For the comparison with the photoemission results it is important to note that in the case of $FeZr_3$ the band calculation yield for the center of the iron d band the energy $\epsilon_d = 0.97$ Ry (marked ϵ_d^{Fe} in Fig. 3). In the case of NiNb in the CuAu structure, the Ni d-band center is at $\epsilon_d^{Ni} = 0.67$ Ry. One observes that, with the exception of NiNb with CsCl structure, the center energy of the late transition metal in the alloy lies in the energy range where the peak in the photoemission spectrum is ob-

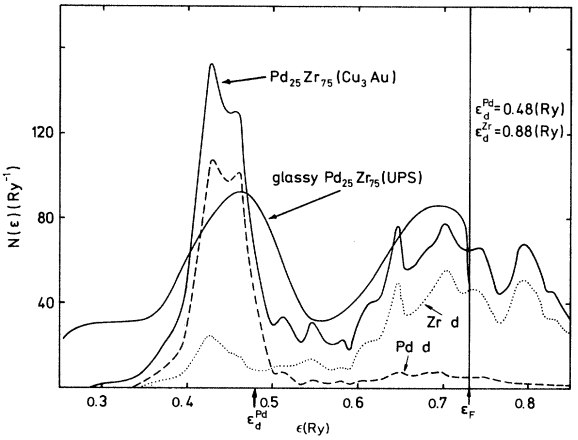

FIG. 1. Results for the total and partial d densities of states $N(\epsilon)$ of $Pd_{25}Zr_{75}$. The experimental photoemission results (Ref. 4) are marked (UPS), the calculated results refer to the ordered compound $PdZr_3$ with Cu_3Au-type symmetry. The peak in the Zr local d density of states $N(\epsilon)$ at $\epsilon \sim (-0.42)$ Ry results from hybridization between Zr and Pd d states. ϵ_d^{Pd} and ϵ_d^{Zr} are d-band-center energies of Pd and Zr, respectively.

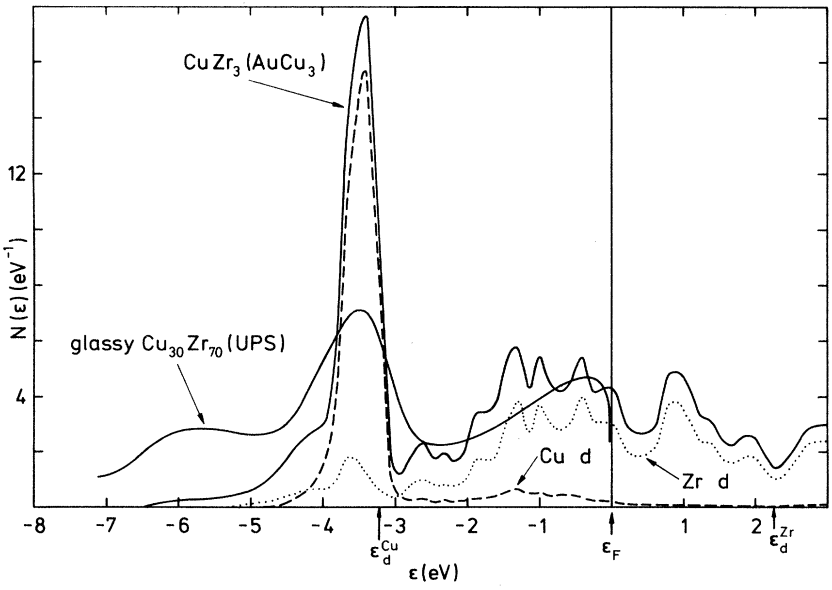

FIG. 2. Results for the total and partial d densities of states, $N(\epsilon)$, of $Cu_{30}Zr_{70}$. The experimental photoemission results (Ref. 4) are marked (UPS), the calculated results refer to the ordered compound $CuZr_3$ with Cu_3Au-type symmetry. ϵ_d^{Cu} and ϵ_d^{Zr} are d-band-center energies of Cu and Zr, respectively.

served.

To interpret the total alloy density of states in terms of the local density of states referring to the alloy constituents A and B, we show in Figs. 1–5 also the d-electron contributions[6] $N_A(\epsilon)$ and $N_B(\epsilon)$ to the total density of states resulting from the A and B atoms, respectively (dashed curves for the late transition element local d-state density and dotted curves for the early transition element).

By comparing $N_A(\epsilon)$ and $N_B(\epsilon)$ with the corresponding density of states of the pure A and B transition metal, one learns how the alloy density of states results from hybridization of the d states of the alloy constituent atoms, from electron charge transfers, and from the change of the Fermi energy ϵ_F. The alloy local density of states $N_A(\epsilon)$ and $N_B(\epsilon)$ are relevant for interpreting soft x-ray experiments, core-level shifts, magnetic properties, etc.

In order to understand the shifts of the d-band centers and the distortions of the shape of the d-band density of states due to alloying and observed in the glassy transition-metal alloys, we compare in Fig. 6 the density of states of glassy $Cu_{40}Zr_{60}$ and crystalline Cu and Zr. The inset illustrates the d-state "repulsion" resulting from hybridization between Cu and Zr d states.[8–10] Figure 6 indicates how such a d-state repulsion causes a narrowing of the Cu d-electron density of states in the alloy. The Cu d states around ϵ^2_{Cu} are more shifted than those around ϵ^1_{Cu} and consequently the Cu d-band peak in $N(\epsilon)$ gets more rounded off and seems to narrow[9] (see Fig. 6).

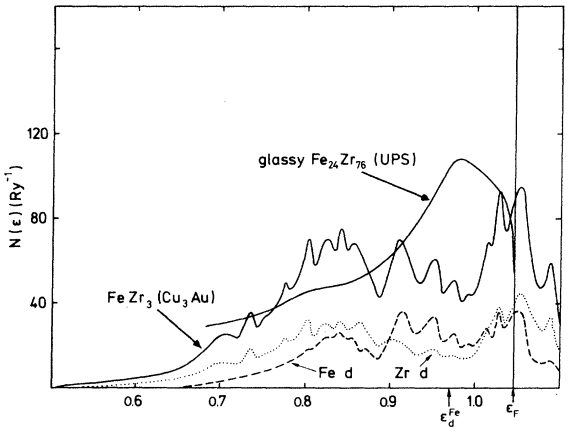

FIG. 3. Results for the total and partial d densities of states, $N(\epsilon)$, of $Fe_{24}Zr_{76}$. The experimental photoemission results (Ref. 4) are marked (UPS), the calculated results refer to the ordered compound $FeZr_3$ with Cu_3Au-type symmetry. ϵ_d^{Fe} is the d-band-center energy of Fe.

To understand the shifts of the d-band centers upon alloying we show in Fig. 7 experimental results[3,4] for the dependence of the density-of-states peak position ϵ_p on alloy composition. For comparison we show also results for $\epsilon_p(x)$ calculated by using $\Delta\epsilon_p = x(\epsilon_F^A - \epsilon_F^B)$. Furthermore,

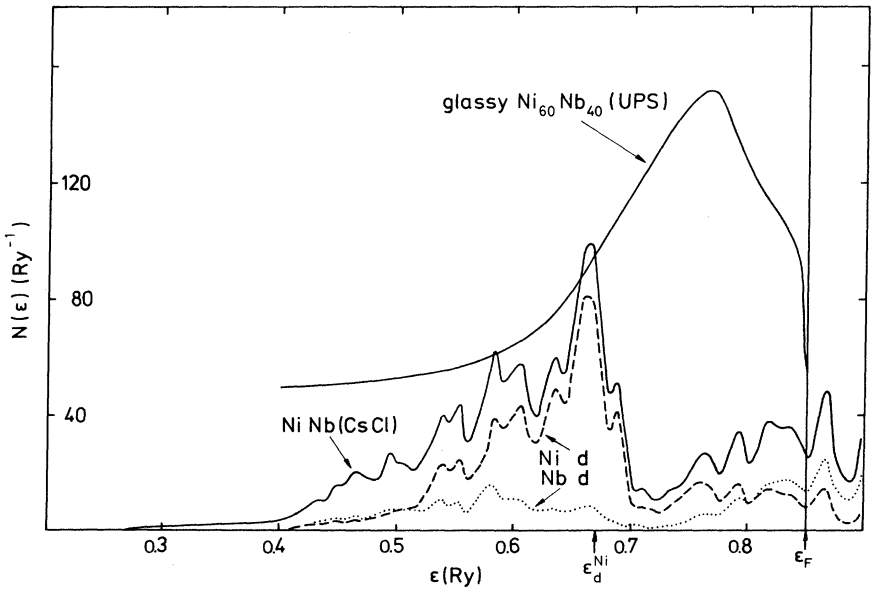

FIG. 4. Results for the total and partial d-electron densities of states, $N(\epsilon)$, of $Ni_{60}Nb_{40}$. The experimental results (Ref. 4) are marked (UPS). The results of the band calculation refer to the ordered compound with CsCl-type symmetry; ϵ_d^{Ni} is the d-band-center energy of Ni.

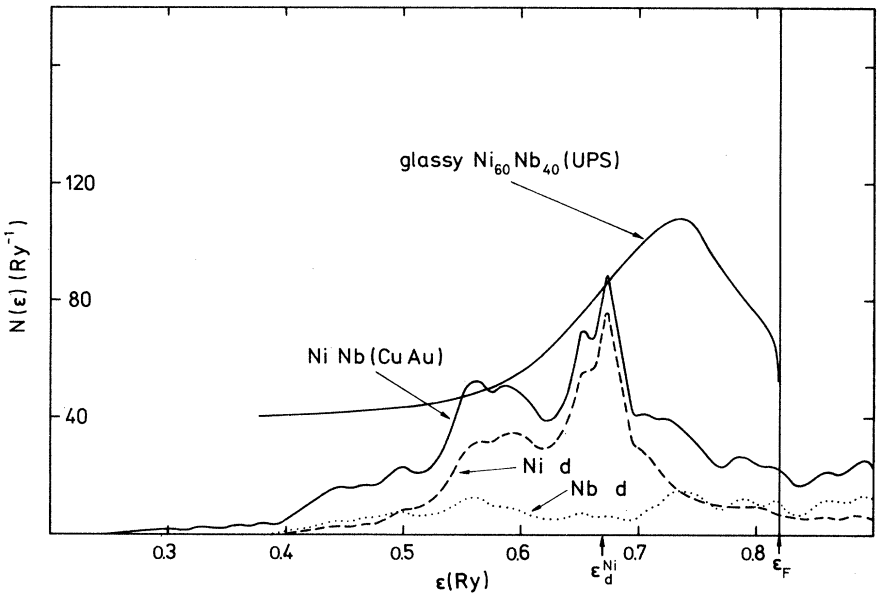

FIG. 5. Same as Fig. 4, except that band calculation refers now to the ordered compound with CuAu-type symmetry.

experimental[4] and calculated[11] results on ϵ_p and its dependence on the valence difference of the alloy constituents are given in Table I.

The large changes in the constituent density of states $N_A(\epsilon)$ and $N_B(\epsilon)$ upon alloying are expected to strongly affect various electronic properties of the alloy. As a result of the d-band shifts and distortion, the screening of the charges of the nuclei changes. Consequently, core-level shifts and changes of the core-level shapes are expected.

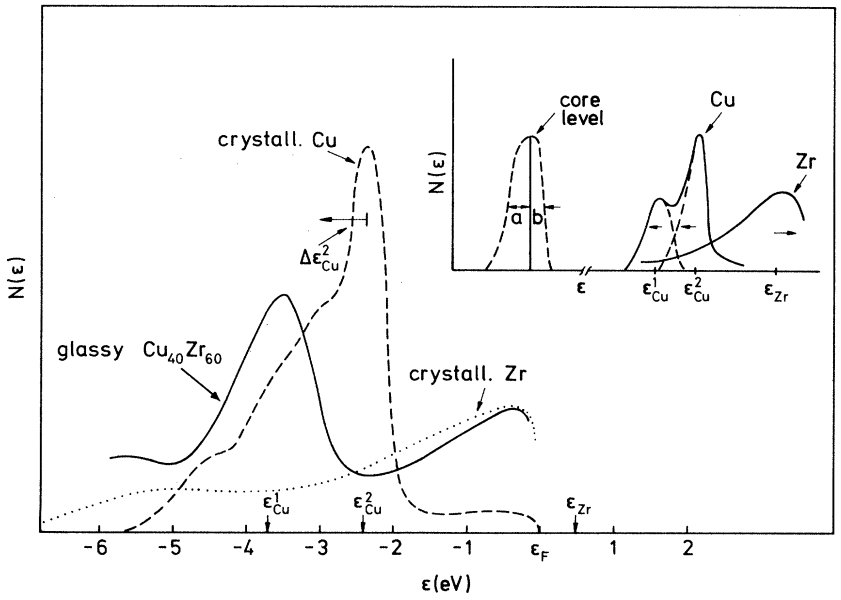

FIG. 6. Experimental results for $N(\epsilon)$ of crystalline Cu and Zr and of glassy $Cu_{40}Zr_{60}$. The peak shift $\Delta\epsilon_{Cu}^2$ due to the change of the Fermi energy and due to the d-state repulsion is estimated to be 0.5 eV. For this calculation we used $\Delta\epsilon_F = x(\epsilon_F^{Zr} - \epsilon_F^{Cu})$ and $(\epsilon_F^{Zr} - \epsilon_F^{Cu})$ was set equal to the difference of the corresponding work function Φ (Φ_{Zr}=3.9 eV, Φ_{Cu} =4.4 eV). The d-state repulsion was calculated by using $t_{CuZr} \simeq 0.4$ eV ($t_{Zr} \simeq 0.6$ eV, $t_{Cu} \simeq 0.3$ eV). The inset illustrates the shifts of the d-band peak positions ϵ_i due to d-state repulsion.

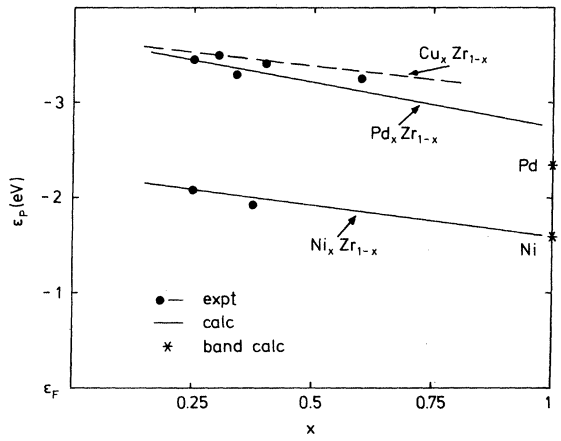

FIG. 7. The concentration dependence of the density-of-states peak position ϵ_p. The calculated results were obtained by using $\Delta\epsilon_p = x(\epsilon_F^A - \epsilon_F^B)$ for the alloys A_xB_{1-x}.

TABLE I. Values for the B-transition-metal d-band peak energy ϵ_p with respect to $\epsilon_F(X)$ in glassy $Zr_{1-x}B_x$ alloys (Ref. 4). Note, $\epsilon_p(X)$ has been calculated by using $\epsilon_p(X) = \epsilon_p(X=1) + \Delta\epsilon_p^1$. Here, $\Delta\epsilon_p^1$ results from the change $\Delta\epsilon_F$ of the Fermi energy. We have neglected the contribution to ϵ_p which results from the covalent d-state repulsion and which, for example, for Cu in $Cu_{40}Zr_{60}$ is of the order of 0.1 to 0.2 eV. For $\epsilon_p(X=1)$ we used results given by Hodges *et al.* (Ref. 11).

B_xZr_{1-x}	ϵ_p^{expt} (eV)	ϵ_p^{calc} (eV)	$\epsilon_p(X=1)$ (eV)	$\Delta\epsilon_p^1$ (eV)
$Cu_{40}Zr_{60}$	3.4	3.3	3.0	0.3
$Ni_{37}Zr_{63}$	1.8	1.98	1.6	0.38
$Co_{40}Zr_{60}$	1.1	0.9	0.6	0.3
$Fe_{30}Zr_{70}$	0.8	0.7	0.5	0.2
$Pd_{25}Zr_{75}$	3.5	3.0	2.3	0.7
$Pt_{21}Zr_{79}$	4.2	4.1	3.0	1.1

B. Core-level shifts and core-level line shapes

Using the theory of Williams and Lang,[13] core-level shifts can be calculated with little additional effort once the electronic structure of an intermetallic compound has been determined. We therefore calculated the core-level shifts for Zr_3Pd, Zr_3Cu, Zr_3Fe, and NiNb and give the results in Table II, where we also list experimental core-level shifts for the glassy transition-metal alloys $Zr_{70}Pd_{30}$, $Zr_{76}Fe_{24}$, and $Ni_{60}Nb_{40}$. Details of the electronic configurations and charge transfer needed for these calculations and the Williams-Lang decomposition of the core-level shifts appear in Table III. The calculated work-function values, Φ, for the alloy $A_{1-x}B_x$ are obtained by interpolating linearly between Φ_A and Φ_B.[16] Table II also contains experimental information [$\delta(a/b)^B$ and $\delta(a/b)^A$] on changes of the core-level line-shape asymmetry $\delta(a/b)$, which is defined in an obvious manner in the inset of Fig. 6. Again, the same information can be obtained theoretically[14] once the electronic-structure changes have been determined. The necessary information is contained in Table IV to determine the sign of $\delta(a/b)$ with[14] $\delta(a/b) \sim \delta N_i(\epsilon_F)$, where $\delta N_i(\epsilon_F)$ denotes the

TABLE II. Core-level asymmetry $\delta(a/b)$ and core-level shifts $\Delta\epsilon_{core}^i$ with respect to the Fermi energy. The experimental results were obtained from XPS core-level spectroscopy (Ref. 12). The calculated results were obtained by using for the work functions $\Phi_{Pd\,Zr_3} = 4.6$ eV, $\Phi_{Cu\,Zr_3} = 4.3$ eV, $\Phi_{Fe\,Zr_3} = 4.4$ eV, and $\Phi_{Ni\,Nb} = 4.5$ eV. The calculated results given in brackets refer to $\Phi_{Pd\,Zr_3} = 4.3$ eV, $\Phi_{Cu\,Zr_3} = 4.5$ eV, $\Phi_{Fe\,Zr_3} = 4.2$ eV, and $\Phi_{Ni\,Nb} = 4.7$ eV obtained by using the work-function values given by Michaelson (Ref. 17). The decrease of $\delta(a/b)$ is indicated by (−) and the increase by (+). (Theoretical results follow from Table IV.)

$A_{1-x}B_x$ Expt.	Theory	$\Delta\epsilon_{core}^B$ (eV) Expt.	Theory	$\delta(a/b)^B$ Expt.	Theory	$\Delta\epsilon_{core}^A$ (eV) Expt.	Theory	$\delta(a/b)^A$ Expt.	Theory
$Zr_{70}Pd_{30}$	Zr_3Pd	-3*d*- 1.5 ± 0.1	1.5 (1.2)	−	−	-3*d*- 0.2 ± 0.1	0.2 (−0.1)	+	+
$Zr_{70}Cu_{30}$	Zr_3Cu	-3*p*-	1.0 (1.2)	−	+	-3*d*-	−0.2 (~0)	−	~0
$Zr_{76}Fe_{24}$	Zr_3Fe	-3*p*- 0 ± 0.2	0.2 (~0)	−	~0	-3*d*- −0.1 ± 0.1	−0.9 (−1.1)	+	~0
$Ni_{60}Nb_{40}$	Ni Nb (CuAu)	-3*d*- 0.5 ± 0.2	0.5 (0.7)	−	−	-3*p*- 0.4 ± 0.2	0.5 (0.7)	−	−

TABLE III. Electron charge transfer and various contributions to core-level shifts $\Delta\epsilon_{core} = \Delta - \Delta_c$ in Zr_3B and NiNb. Here, Δ and Δ_c refer to the pure metal and compound, respectively. $\Delta = \Delta_{conf} + \Delta_{relax} + \Delta_{chem}$. The values in parentheses are obtained by calculating work function Φ from the Φ_A, Φ_B values given by Michaelson (Ref. 17).

	Occupation n_s+n_p	Occupation n_d	Δ_{conf} (eV)	Δ_{relax} (eV)	Δ_{chem} (eV)		Δ_c (eV)	
Pd (metal)	1.2	8.8	−5.6	5.7	1.2		1.3	
Zr (metal)	1.3	2.7	2.5	4.0	1.0		7.5	
Pd in $PdZr_3$	1.8	8.8	−0.3	3.6	−3.5	(−3.2)	−0.2	(0.1)
Zr in $PdZr_3$	1.1	2.7	−0.2	4.4	3.1	(3.4)	7.3	(7.6)
Cu (metal)	1.5	9.5	−3.0	0.3	6.8		4.1	
Zr (metal)	1.3	2.7	2.5	4.0	1.0		7.5	
Cu in $CuZr_3$	2.4	9.6	4.9	3.5	−5.3	(−5.5)	3.1	(2.9)
Zr in $CuZr_3$	1.0	2.66	−0.6	4.4	3.9	(3.7)	7.7	(7.5)
Fe (metal)	1.4	6.6	3.4	5.8	0.0		9.2	
Zr (metal)	1.3	2.7	2.5	4.0	1.0		7.5	
Fe in $FeZr_3$	1.8	7.1	12.4	2.6	−6.0	(−5.8)	9.0	(9.2)
Zr in $FeZr_3$	0.9	2.8	0.0	4.3	4.1	(4.3)	8.4	(8.6)
Ni (metal)	1.4	8.6	3.8	6.3	0.2		10.3	
Nb (metal)	1.3	3.7	−1.0	4.4	1.2		4.6	
Ni in NiNb	1.9	8.8	9.0	4.1	−3.3	(−3.5)	9.8	(9.6)
Nb in NiNb	1.0	3.3	−8.0	5.2	6.9	(6.7)	4.1	(3.9)

change of the local density of states at ϵ_F of the atoms of sort i. The above expression for the change of the core-level shape asymmetry is in accordance with the results[14] that the core-level asymmetry arises from electron-hole excitations and is proportional to the local density of states $N_i(\epsilon_F)$ $(i = A, B)$.

III. DISCUSSION

First, we comment on the shifts of the d-band centers and the d-band shape distortion in the density of states $N(\epsilon)$ observed for the glassy transition-metal alloys. As shown in Figs. 1–5 the overall shape of $N(\epsilon)$ in the glassy transition-metal alloys observed in the photoemission spectra and of $N(\epsilon)$ calculated for hypothetical close-packed ordered compounds of approximately the same stoichiometry is similar. Of course, fine structure in $N(\epsilon)$ due to crystal symmetries is lost in the amorphous alloy, but the peak positions and widths are approximately the same. Note, for all alloys shown in Figs. 1–5 the peak in the intensity of the photoemission spectrum occurs at energies coinciding with the center energy of the late transition-metal d band. Also, note that the UPS cross section for Fe $3d$ states and other $3d$ states and Zr $4d$ states may differ. Keeping this in mind and also that in contrast to the ordered compounds in the glassy alloys, variations of atomic distances and coordination number are expected, one may conclude that the density of states calculated for ordered compounds are in satisfactory agreement with the photoemission spectra observed for the corresponding glassy alloys. Thus, we must conclude that the electronic structure in the glassy state is similar to the electronic structure of an ordered close-packed state.

TABLE IV. Calculated results for the electron density of states at ϵ_F in units of Ry^{-1} per atom. (a) indicates results obtained by the ASW method. (b) indicates results obtained by Moruzzi *et al.* (Ref. 18).

Metal	$N(\epsilon_F)$ (a)	$N(\epsilon_F)$ (b)	Compound A	Compound B	$N_A(\epsilon_F)$ (a)	$N_B(\epsilon_F)$ (a)
Fe	43	42	$FeZr_3$		42	17
Ni	42.5	55	NiNb		10	12
Cu	3.5	3.9	$CuZr_3$		8	17
Pd	30	31	$PdZr_3$		10	19
Zr	18	17.5				
Nb	18	19				

The decomposition of the total density of states $N(\epsilon)$ into the local density of states $N_A(\epsilon)$ and $N_B(\epsilon)$ of the alloy constituents shows that large shifts of the peaks in $N(\epsilon)$ of the late transition metal occur. These shifts result from the change of the Fermi energy from the hybridization of the d states of the alloy constituents and from electron charge transfer between the alloy atoms A and B. For a qualitative discussion the shifts due to d state repulsion[9] caused by the additional d-state hybridization in the alloy may be approximately described by

$$\epsilon_{1,2} = \tfrac{1}{2}(\epsilon_A + \epsilon_B) \pm \tfrac{1}{2}[(\epsilon_A - \epsilon_B)^2 + 4t^2]^{1/2}.$$

Here, ϵ_i $(i = A, B)$ refer to the center of gravity

energies of the A- or B-atom d bands and the hopping integral t refers to d-electron transitions between atoms A and B. In the nearly-split-band limit the above expression fairly well describes the shifts of the d-band centers due to hybridization. Note, the above treatment of hybridizational shifts may be refined considerably as indicated in Fig. 6 by decomposing $N(\epsilon)$ into Lorentzian-type peaks with centers of gravity ϵ_A^1, ϵ_A^2, etc., and then by calculating the covalent splitting of ϵ_A^1 and ϵ_B^1 (1 = 1, 2, etc.) according to the above simple formula. This d-state repulsion is nearly independent of alloy composition and causes, as indicated in the inset of Fig. 6, an upward shift of the Zr d band and a downward shift of the late transition-metal d states and also a narrowing of the latter d band. As indicated in Fig. 6 the Cu d states around ϵ_{Cu}^2 are more shifted than those around ϵ_{Cu}^1 and consequently the Cu d band gets more rounded off and seems to narrow as is observed. In Table V results are given for the shift and narrowing of the Cu d band due to hybridization in the case of $Cu_{40}Zr_{60}$.

In addition to the shifts due to hybridization discussed above, shifts of the d-band-center energy results from the change in the Fermi energy which is approximately determined by $\epsilon_F(x) = (1 - x)\epsilon_F^A + x\epsilon_F^B$ provided that interatomic electronic charge transfer is not too large. Note, $(\epsilon_F^A - \epsilon_F^B)$ may be equated to the corresponding difference in work function. From the results show in Fig. 7 and Table I, one concludes that the concentration and valence dependence of the late transition-metal peak shift $\delta\epsilon_p$ results mainly from the corresponding changes of $\epsilon_F(x)$ and of[11] $(\epsilon_F^B - \epsilon_p)$.

The core-level shifts arise from intra-atomic $s \rightarrow d$ and interatomic electron charge transfer.[13] Core levels get more strongly bound due to poorer screening of the atomic core potentials. Except for Zr in $FeZr_3$ it is apparent from Table II that the agreement between the calculated core-level shifts and the observed shifts is quite satisfactory. Thus, one again concludes that the electronic configuration in the glassy alloys and corresponding close-packed ordered systems is similar. To eliminate uncertainties in the calculations resulting from not knowing the alloy work-function values too well, it would be very useful to determine experimentally the work functions of the glassy alloys studied here.

For a physical interpretation of the core-level shifts ϵ_i, first note that they are measured with respect to the alloy Fermi energy. Therefore, the core-level shifts may be decomposed as

$$\Delta\epsilon_i = \Delta\epsilon_i^1 + \Delta\epsilon_i^2 ,$$

where $\Delta\epsilon_i^1$ results from the change in the Fermi energy and $\Delta\epsilon_i^2$ from the distortion of $N(\epsilon)$, respectively, from the redistribution of electrons upon alloying. The contribution $\Delta\epsilon_i^2$ may be written as[14]

$$\Delta\epsilon_i^2 = (U_{is} - U_{id})\,\Delta n_s + \delta .$$

The first term results from intra-atomic s-d charge transfer and U_{is} and U_{id} describe the effective Coulomb interaction between electrons in the core-state i, and s- and d-conduction electron states. Δn_s is the change in the number of s electrons within the atomic cell due to the intra-atomic s-d charge transfer. The core-level shift δ results from interatomic electron charge transfer. Due to the stronger Coulomb interaction between core- and d-conduction electrons than core- and s-conduction electrons, the intra-atomic $d \rightarrow s$ charge transfer leads to a stronger binding of core electrons. Due to the repulsive electron-electron interaction in the interatomic charge transfer into an atomic cell, this leads to a decrease of core-electron binding within that cell. However, the corresponding Madelung energy produces a shift in the opposite direction. Thus, stronger binding of core states will occur at such atoms, where alloying causes intra-atomic $d \rightarrow s$ charge transfer and where the interatomic electron charge flows out of that atomic cell. Stronger binding of the corelevels occurs also if electron charge flows into the atomic cell, as long as the stronger binding due to intra-atomic $d \rightarrow s$ electron redistribution and Madelung-type energy attraction dominates. On the basis of the

TABLE V. Experimental and calculated values for the Cu d-band distortion in $Cu_{40}Zr_{60}$. The shift $\Delta\epsilon_{\mathrm{Cu}}^2$ of the Cu low-binding d-band peak position is calculated by using $\Delta\epsilon_{\mathrm{Cu}}^2 = (\Delta\epsilon_{\mathrm{Cu}}^2)_1 + (\Delta\epsilon_{\mathrm{Cu}}^2)_2$. Here $(\Delta\epsilon_{\mathrm{Cu}}^2)_2 \simeq 0.15$ eV results from the d-state repulsion between the hybridizing Cu and Zr d states and $(\Delta\epsilon_{\mathrm{Cu}}^2)_1 = X(\epsilon_F^{\mathrm{Zr}} - \epsilon_F^{\mathrm{Cu}}) = 0.3$ (eV) from the change of the Fermi energy. $W_p \simeq \sqrt{Z_1}\,t$ is the Cu peak width, which should be corrected by the peak narrowing $[(\Delta\epsilon_{\mathrm{Cu}}^2)_2 - (\Delta\epsilon_{\mathrm{Cu}}^1)_2] \approx 0.1$ (eV) due to d-state repulsion. Z_1 is the number of NN Cu atoms around a Cu atom in the alloy.

$Cu_{40}Zr_{60}$	$\Delta\epsilon_{\mathrm{Cu}}^2$ (eV) – expt.	$\Delta\epsilon_{\mathrm{Cu}}^2$ (eV) – calc.	W_p^{expt} (eV)	W_p^{calc} (eV)
Cu	0.9	~0.5	1.0	~0.7

electronegativity scale, we expect in the studied alloys interatomic electron charge transfer from Zr to Ni, Fe, Pd, etc. Furthermore, the hybridization of the stronger bound d states of Ni, Fe, Pd, etc. with the Zr d states should cause an $s \rightarrow d$ intra-atomic charge transfer at Ni, Fe, Pd, etc. atomic sites. For example, in the case of Zr_3Pd our calculation shows that Pd atoms receive 0.6 s and p electrons from the Zr atoms which loose 0.20 electrons (see Table III). Furthermore, the $s \rightarrow d$ charge transfer at Pd sites is calculated to be nearly zero. Consequently, we expect stronger binding of Zr core electrons. At Pd sites the core-level shifts due to the interatomic electron charge transfer cause a weaker binding of the core level. However, the energy shift due to the surrounding attractive Zr core potentials or corresponding Madelung-Coulomb energy is larger and causes a stronger binding of the Pd core level. As a result of this and of the increase in Fermi energy with respect to ϵ_F(Pd), one obtains for ϵ_{3d} a net stronger binding by 1.5 eV. The other results for the core-level shifts should be interpreted in the same way.

The asymmetry $\delta(a/b)$ as defined in the inset of Fig. 6 of the core levels is expected to increase if $N_i(\epsilon_F)$ increases, and to decrease if $N_i(\epsilon_F)$ decreases.[15] Consequently, from our calculations of $N_A(\epsilon)$ and $N_B(\epsilon)$ in Table IV we must conclude that the core-level asymmetry of the late transition metals in glassy $Zr_{1-x}B_x$ alloys should decrease as is observed (see Table II). Due to the upward shift of the Zr d states we expect a slight increase of $\delta(a/b)$ for Zr, again in agreement with experiment. Since for Cu in $Zr_{1-x}Cu_x$ one observes $N^d_{Cu}(\epsilon_F) \approx 0$, one expects small changes of $\delta(a/b)$ for Cu.

We finally turn to the dependence of the glass-forming ability and the stability of the glass on electronic parameters. This is a problem of particular importance which we do not claim to solve. But, to shed light on this problem, we show in Fig. 8 results for the crystallization temperature T_{cryst} for various transition-metal alloys. One sees that T_{cryst} depends linearly on valence difference ΔN of the alloy constituents and on the heat of formation ΔH,

$$T_{cryst} \sim \delta \Delta H .$$

To explain this linear dependence we assume that the thermal stability of the amorphous transition-metal alloys results essentially from the strain energy ΔU associated with the migration of the (smaller) atoms, which is necessary for recrystallization. Since in $Zr_{1-x}B_x$ the atomic volume of the B atoms (Cu, Ni, Co, ...) is nearly the same, this atomic migration requires approximately the same local volume changes or $A-B$ bond-length changes. Therefore, $\Delta U \propto \Delta H$, where ΔH is the alloy heat of formation which is a measure for the $A-B$ bond energy. Since the entropy due to configurational atomic disorder should not vary much for different B atoms, we have for the free-energy change $\delta \Delta F \simeq \delta \Delta U$, and thus for the change δT_{cryst} of the crystallization temperature, $\delta T_{cryst} \propto \delta \Delta U$. Here, $\delta \Delta F$, $\delta \Delta U$, etc. denote the change resulting from changing the B atoms. Thus, the recrystallization temperature should

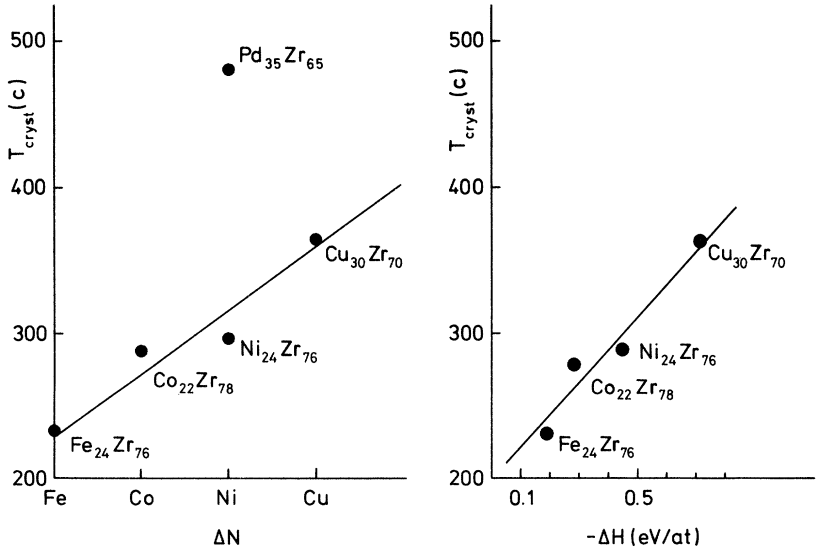

FIG. 8. The crystallization temperature T_{cryst} as a function of the heat of formation ΔH and of the valence difference ΔN of the two alloy constituents. The results refer to $Zr_{1-x}B_x$-type alloys with B = Cu, Ni, etc.

vary as

$$T_{\text{cryst}} \propto \delta \Delta H .$$

Due to d-energy mismatch,[1] ΔH increases with increasing valency of the B atoms in $Zr_{1-x}B_x$ alloys, and thus T_{cryst} as well as the glass temperature T_g increases with the valence difference ΔN between Zr and B atoms. This explains the results shown in Fig. 8. It is interesting to note that T_{cryst} of PdZr does not lie on the linear curve $T_{\text{cryst}}(\Delta H)$ obtained for $Zr_{1-x}B_x$, with B atoms having the same atomic volume. This is expected on the basis of our explanation since Pd has a larger volume than the other B atoms. Note, in alloys $Zr_{1-x}Ni_x$ one expects[2] that $T_{\text{cryst}}(x) \sim \delta \Delta H(x)$. Hence, the concentration dependence of T_{cryst} should mainly result from $\Delta H(x)$.

Incidentally, we suspect that the glass-forming ability of AB alloys requires a difference in atomic volume. Note, it seems impossible to form pure amorphous transition metals. Maybe due to the volume relaxation in the glass, the strain energy resulting from different atomic volume is lowered upon atomic disorder. This may not apply to simple s,p-type glasses.

It should be noted that in the case of transition-metal–metalloid glasses our arguments presented here will not directly apply. It is possible that in $Fe_{80}B_{20}$, etc. the transition from the crystalline to the amorphous states involves a weakening of d bonds and a strengthening of d–p and s–p bonds, and the latter may depend more strongly also on bond direction.[16] Consequently, the changes of electronic and atomic structure may be different from what occurs for amorphous transition-metal alloys.

ACKNOWLEDGMENTS

We thank Dr. R. de Groot for useful discussions on core-level shifts. We also like to thank Ms. Brück for technical help with some of the band-structure calculations.

[1] A. R. Williams, C. D. Gelatt, Jr., and V. L. Moruzzi, Phys. Rev. Lett. 44, 429 (1980); R. E. Watson and L. H. Bennett, Phys. Rev. B 18, 6439 (1978).
[2] K. H. J. Buschow and N. M. Beekmans, Phys. Rev. B 19, 3843 (1979).
[3] P. Oelhafen, E. Hauser, H.-J. Güntherodt, and K. H. Bennemann, Phys. Rev. Lett. 43, 1134 (1979).
[4] P. Oelhafen *et al.*, unpublished.
[5] M. Liard, T. Laubschar and H. Kunzi, private communication.
[6] A. R. Williams, J. Kübler, and C. D. Gelatt, Phys. Rev. B 19, 6094 (1979).
[7] L. Hedin and B. I. Lundqvist, J. Phys. C 4, 2064 (1971).
[8] J. Friedel, in *The Physics of Metals*, edited by J. M. Ziman (Cambridge University Press, London, 1969).
[9] V. L. Moruzzi, A. R. Williams, and J. F. Janak, Phys. Rev. B 10, 4856 (1974); J. Kübler, J. Phys. F 8, 2301 (1978).
[10] S. Kirkpatric, B. Velicky, and H. Ehrenreich, Phys. Rev. B 1, 3250 (1970).
[11] L. Hodges, R. E. Watson, and H. Ehrenreich, Phys. Rev. B 5, 3953 (1972).
[12] P. Oelhafen *et al.*, unpublished.
[13] A. R. Williams and N. D. Lang, Phys. Rev. Lett. 40, 954 (1978).
[14] R. M. Friedman *et al.*, Phys. Rev. B 8, 2433 (1973).
[15] P. Ascarelli, Solid State Commun. 21, 205 (1977).
[16] M. Matsuura *et al.*, Solid State Commun. 33, 895 (1980).
[17] A. Michaelson, J. Appl. Phys. 48, 4729 (1977).
[18] V. L. Moruzzi *et al.*, in *Calculated Electronic Properties of Metals* (Pergamon, New York, 1971).